CD38 Deficiency Protects Mouse Retinal Ganglion Cells Through Activating the NAD+/Sirt1 Pathway in Ischemia-Reperfusion and Optic Nerve Crush Models

Yulian Pang,[1] Haijian Hu,[1] Ke Xu,[1] Ting Cao,[1–3] Zhiruo Wang,[1,4] Jiahe Nie,[1,5] Haina Zheng,[1] Hongdou Luo,[1] Feifei Wang,[1] Chan Xiong,[1] Ke-Yu Deng,[6] Hong-Bo Xin,[6] and Xu Zhang[1]

[1]Affiliated Eye Hospital of Nanchang University, Jiangxi Medical College, Nanchang University, Jiangxi Research Institute of Ophthalmology and Visual Science, Jiangxi Provincial Key Laboratory for Ophthalmology, Jiangxi Clinical Research Center for Ophthalmic Disease, Nanchang, China
[2]Department of Orthopaedics, The Fourth Medical Center of Chinese PLA General Hospital, Beijing, China
[3]Medical School of Chinese PLA, Beijing, China
[4]Department of Ophthalmology, The Second Xiangya Hospital of Central South University, Changsha, China
[5]State Key Laboratory of Ophthalmology, Zhongshan Ophthalmic Center, Sun Yat-Sen University, Guangdong Provincial Key Laboratory of Ophthalmology and Visual Science, Guangzhou, China
[6]Institute of Translational Medicine, Nanchang University, Nanchang, China

Correspondence: Xu Zhang, Affiliated Eye Hospital of Nanchang University, 463 Bayi Road, Nanchang 330006, China; xuzhang19@163.com.
Hong-Bo Xin, Institute of Translational Medicine, Nanchang University, Nanchang 330047, China; xinhb@ncu.edu.cn.

YP, HH and KX contributed equally to this work.

Received: December 27, 2023
Accepted: May 5, 2024
Published: May 22, 2024

Citation: Pang Y, Hu H, Xu K, et al. CD38 deficiency protects mouse retinal ganglion cells through activating the NAD+/Sirt1 pathway in ischemia-reperfusion and optic nerve crush models. *Invest Ophthalmol Vis Sci.* 2024;65(5):36. https://doi.org/10.1167/iovs.65.5.36

Purpose. The purpose of this study was to investigate the protective effect of CD38 deletion on retinal ganglion cells (RGCs) in a mouse retinal ischemia/reperfusion (I/R) model and an optic nerve crush (ONC) model, and to elucidate the underlying molecular mechanisms.

Methods. Retinal I/R and ONC models were constructed in mice. PCR was used to identify the deletion of CD38 gene in mice, hematoxylin and eosin (H&E) staining was used to evaluate the changes in retinal morphology, and electroretinogram (ERG) was used to evaluate the changes in retinal function. The survival of RGCs and activation of retinal macroglia were evaluated by immunofluorescence staining. The expression of Sirt1, CD38, Ac-p65, Ac-p53, TNF-α, IL-1β, and Caspase3 proteins in the retina was further evaluated by protein imprinting.

Results. In retinal I/R and ONC models, CD38 deficiency reduced the loss of RGCs and activation of macroglia and protected the retinal function. CD38 deficiency increased the concentration of NAD+, reduced the degree of acetylation of NF-κB p65 and p53, and reduced expression of the downstream inflammatory cytokines TNFα, IL-1β, and apoptotic protein Caspase3 in the retina in the ONC model. Intraperitoneal injection of the Sirt1 inhibitor EX-527 partially counteracted the effects of CD38 deficiency, suggesting that CD38 deficiency acts at least in part through the NAD+/Sirt1 pathway.

Conclusions. CD38 plays an important role in the pathogenesis of retinal I/R and ONC injury. CD38 deletion protects RGCs by attenuating inflammatory responses and apoptosis through the NAD+/Sirt1 pathway.

Keywords: retinal ganglion cells (RGCs), CD38, NAD+, Sirt1, inflammation, apoptosis

Glaucoma is currently considered a multifactorial, progressive neurodegenerative disorder characterized by the death of retinal ganglion cells (RGCs) involved in constituting the optic nerve. These ultrastructural changes gradually develop and clinically lead to visual impairment and changes in quality of life with increasing optic disc depression and consequent specific and irreversible visual field (VF) defects.[1] As with many neurodegenerative diseases, dysfunction in mouse models of glaucoma is associated with neuroinflammation and glial cell activation.[2,3] In acute optic nerve injury and chronic neurodegenerative diseases, microglial activation and macrophage infiltration can be accompanied by the release of large amounts of inflammatory cytokines from the retina and proximal optic nerve, ultimately leading to extensive neuronal loss and axonal degeneration.[4] Moreover, some inflammatory factors can induce neurotoxic reactive astrocytes to release toxins to specifically kill neurons.[5,6]

As an important member of the Sirtuin family of deacetylases dependent on nicotinamide adenine dinucleotide (NAD+), Sirt1 has anti-apoptotic, anti-inflammatory, and anti-aging effects, and regulates cell transcription and energy metabolism.[7,8] Its protective effects are mainly achieved by increasing deacetylation or adenosine diphosphate (ADP) ribosylation of antioxidant pathways and related proteins to promote DNA damage repair.[9,10] Among them, the

deacetylase action of Sirt1 is the focus of this study. On the one hand, Sirt1 can directly interact with and deacetylate the RelA/p65 subunit of the NF-κB complex, thus playing an important role in the termination of NF-κB-driven inflammatory responses and enhancing the resolution of inflammation.[11] On the other hand, Sirt1 can inhibit p53 activity through deacetylation, thereby inhibiting p53-dependent apoptosis and senescence and promoting cell survival.[12] NAD+ is an essential cofactor for the nonredox NAD+ -dependent enzyme SIRT1. Many studies describe an important role for NAD+ in neurodegeneration.[13] Indeed, NAD+ was found to be an effective neuroprotective and anti-inflammatory molecule,[14] yet its levels were found to decrease with age.[15] In 2016, it was discovered that the expression of CD38, the main enzyme leading to NAD+ degradation, increased with aging, thus explaining the age-related decline in NAD.[16] CD38, a 45 kDa transmembrane glycoprotein, is the major hydrolytic enzyme that degrades NAD+ and is expressed in many tissues.[17] CD38 knockout (KO) mouse brains showed a 10-fold increase in NAD+ levels compared to wild-type mice, suggesting that CD38 is one of the major modulators of intracellular NAD+ levels in the brain.[18] In addition, silencing CD38 expression using siRNA increased NAD+ levels 5-fold in rat cortical neuron cultures, an effect that was accompanied by a 5-fold increase in the activity of the NAD-dependent enzyme SIRT1.[19] Thus, the CD38 mediated NAD+/Sirt1 pathway may play an important role in central nervous system protection. Although CD38 has been largely studied in other tissues and organs throughout the body, CD38 research in ophthalmology, especially in glaucoma neuroprotection, remains very scarce.

Our team has previously demonstrated CD38 expression and localization in the retina.[20] Combined with previous research results, this study will investigate the regulatory effect of CD38 deletion on RGC survival and neuroinflammation in common glaucoma injury models, namely the optic nerve crush (ONC) model and ischemia/reperfusion (I/R) model, and indicate that this regulation is at least partially mediated through NAD+/Sirt1.

Materials and Methods

Animals

Eight-week-old, wild-type and CD38 KO ($CD38^{-/-}$) male mice (C57BL/6 background) were used in the experiments. $CD38^{-/-}$ mice were obtained from Dr. Frances E. Lund (Rochest). Additional male Sprague-Dawley (SD) rats aged 2 to 3 months and weighing between 250 and 300 g were obtained from the Laboratory Animal Science Center of Nanchang University. The mice and rats were housed under conditions of controlled temperature (22–24°C) and illumination (12-hour dark/light cycle) with free access to water and food. All experiment procedures using animals were performed in accordance with regulations set by the Animal Care and Use Committee of Nanchang University and the ARVO Statement for the Use of Animals in Ophthalmic and Vision Research. The study was approved by the Medical Research Ethics Committee of Affiliated Eye Hospital of Nanchang University (protocol number: YLP20221202) before its onset. All efforts were made to minimize animal suffering and reduce the number of animals used for the experiments.

Transient Retinal Ischemia/Reperfusion Model

A retinal I/R model was induced as described previously.[7] The mice were first anesthetized using an intraperitoneal injection of 1% (w/v) sodium pentobarbital (50 mg/kg).[21] Following mydriasis with tropicamide and local anesthesia with oxybuprocaine, a 32G injection needle connected to saline was inserted into the anterior chamber. The saline reservoir was elevated, and the intraocular pressure (IOP) was raised to 110 mm Hg in the left eye for 60 minutes. The other eye was used as a control by inserting a needle and maintaining normal IOP.[22,23] We used the Tonopen tonometer to measure bilateral eye IOP.

ONC Procedure and Drug Administration

The mice were anesthetized as previously described. Surgery was performed as described by Puyang et al.[24] A small incision was made in the superior and lateral conjunctiva, blunt dissection was performed gently to expose the optic nerve and avoid bleeding, and next, the optic nerve was squeezed 1 to 2 mm behind the eyeball for 10 seconds using fine forceps (Dumont5B; WPI, Sarasota, FL, USA). In the contralateral eye, the same procedure was performed as in the control group without optic nerve clamping. EX527 (Med Chem Express, Monmouth Junction, NJ, USA) was injected into the peritoneal cavity of $CD38^{-/-}$ mice to suppress SIRT1 activity. EX527 was injected intraperitoneally at a dose of 10 mg/kg from the day of the ONC procedure, and the control group received the same amount of phosphate-buffered saline (PBS).[21] Animals received this treatment for 7 consecutive days. Euthanasia was performed with an overdose of sodium pentobarbital on postoperative day 7 and samples were collected for histological analysis.

Gene Identification

Total DNA was extracted from mouse tails according to the manufacturer's protocol. To identify the mouse genotype, the following primers were used: Forward: 5′-CATAGTGAACGGATTGTTATCTG-3′, and Reverse: 5′-AGATGGAGACTGACCTAGGAGG-3′. The cycling parameters were: initial denaturation (95°C for 5 minutes), 20 cycles (95°C for 30 seconds, 65°C for 30 seconds, and 72°C for 30 seconds), then 20 cycles (95°C for 30 seconds, 55°C for 30 seconds, and 72°C for 30 seconds) and then an extension step (72°C for 3 minutes). The amplified DNA was then electrophoresed in a 3% agarose gel (with ethidium bromide) and analyzed by Image Lab under UV light. We use a DNA ladder (D526A, TAKARA, Japan) to identify the DNA band sizes.

Electroretinogram

Anesthetized with 1% (w/v; 50 mg/kg) sodium pentobarbital, the mice were subjected to dim red light following overnight dark adaptation (> 12 hours). Then, the pupils were dilated with 1% tropicamide. A reference electrode was placed at the midpoint of the line between the eye and ear and a grounding electrode was placed near the tail. Adult mice ($n = 3$) were subjected to the guidelines of the International Society for Clinical Electrophysiology of Vision (ISCEV), including the scotopic 3.0 electroretino-

Investigative Ophthalmology & Visual Science

Table. Primary Antibodies Used in the Study

Antibody	Supplier	Catalog No.	Host	Dilution
GAPDH	Tran. lab	HC301	Mouse mAb	1:2500 (WB)
CD38	R&D	Cbvd0120081	Sheep mAb	1:500 (WB)
Sirt1	CST	9475	Rabbit mAb	1:1000 (WB)
Rbpms	Abcam	Ab152101	Rabbit polyclonal	1:100 (IF)
GFAP	Sigma	g-2893	Mouse mAb	1:100(IF),1:1000 (WB)
Ac-p65	Cell Signaling	#3045S	Rabbit mAb	1:1000 (WB)
Ac-p53	Cell Signaling	2570S	Rabbit mAb	1:1000 (WB)
TNF-α	Wanleibio	WL01581	Rabbit polyclonal	1:1000 (WB)
IL-1β	Wanleibio	WL00891	Rabbit polyclonal	1:1000 (WB)
Caspase3	Wanleibio	WL02117	Rabbit mAb	1:500 (WB)
CD38	Santa Cruz	sc-374650	Mouse mAb	1:100 (IF)
GS	Abcam	AB64613	Mouse mAb	1:100 (IF)

Ac-p65, Acetylated p65; Ac-p53, Acetylated p53; Caspase3, cysteinyl aspartate specific proteinases 3; CD38, recombinant cluster of differentiation 38; GAPDH, glyceraldehyde-3-phosphate dehydrogenase; GFAP, glial fibrillary acidic protein; GS, Glutamine Synthetase; IF, immunofluorescence; IL-1β, Interleukin-1β; Rbpms, RNA-Binding Protein with Multiple Splicing; Sirt1, recombinant sirtuin 1; TNF-α, tumor necrosis factor α; WB, Western blot assay.

gram (ERG) test (cone and rod response) elicited by white light flashes at an intensity of 3.0 phot cd s/m^2, the scotopic 3.0 OPS test (oscillatory potentials) simultaneously elicited by white light flashes at an intensity of 20.0 phot cd s/m^2, photopic 3.0 ERG test (cone response) under a white background elicited by white light flashes at an intensity of 2.8 phot cd s/m^2, and under a white background light at 29.0 phot cd/m^2 after 10 minutes of light adaptation. The amplitude of the a-wave was measured from the baseline to the trough, whereas that of the b-wave was measured from the maximum of the a-wave trough to the peak of the b-wave.

Immunofluorescence

Eyeballs were separated, fixed, dehydrated, and embedded in paraffin blocks and cut into 5-µm sections. For ease of analysis, all eye sections were selected from the central region of the eye through the optic nerve head. Following deparaffinization, sections were heated in 10 mM sodium citrate buffer (pH 6.0) for 10 minutes and then chilled for 30 minutes for antigen retrieval. Tissues were blocked with PBS containing serum and 0.1% Triton X-100 for 1 hour at room temperature. Tissues were incubated with primary antibody (see the Table) and left overnight at 4°C. Secondary antibodies were donkey-anti-mouse-Alexa Flour 594 and donkey-anti-mouse-Alexa Flour 488 incubated for 1 hour at room temperature and washed. Nuclei were then stained with DAPI (Vector Laboratories, Inc., Burlingame, CA, USA) and mounted under coverslips. Staining was observed using a confocal microscopy at a magnification of × 20 (Axio – Imager LSM – 800, Zeiss, Germany).

Hematoxylin and Eosin Staining

Paraffin sections of eyeballs were prepared as described above and then deparaffinized with xylene solution and graded concentrations of ethanol (100%, 95%, 80%, and 70%). Tissues were stained with hematoxylin and eosin (H&E) and observed under a light microscope (Leica, Heidelberg, Germany). Retinal thickness was measured at each quarter point of each retinal cross-section on HE sections using Image Pro Plus version 6.0 (Media Cybernetics) and then averaged.

RGC Counting

Mouse eyes were enucleated on day 3 after I/R and day 7 after ONC and fixed in 4% paraformaldehyde (PFA). One hour later, the sclera was carefully dissected and the retina was dissected and cut into four quadrants to form four flaps that were flattened on a glass slide. After blocking with PBS containing 1% Triton X-100 (Solarbio, Beijing, China) and 5% donkey serum (Gibco, Australia), incubation with primary antibodies (Rbpms) was performed overnight at 4°C. They were washed 3 times in PBS and then incubated with secondary antibody (donkey-anti-rabbit AlexaFlour 488) at 1:200 for an additional 1 hour at room temperature. Following washing, the retinas were imaged using a confocal microscope (Zeiss, LSM800, Germany). Images were acquired at peripheral (approximately 150–200 µm from the retinal edge), middle (approximately 700–800 µm from the edge), and central (approximately 1500–1600 µm from the edge) locations in each quadrant.[25] A total of 12 images were collected per retina and RBPMS positive cells were counted in a blinded manner.

Western Blot Analysis

Retinal tissues were dissected and rinsed with PBS. The samples were lysed with RIPA buffer containing phenylmethylsulfonyl fluoride (PMSF; Solarbio, China) on ice for 30 minutes after the ultrasonic break. Protein concentrations were measured using the Bradford assay (Beyotime Institute of Biotechnology). Sample proteins (30 µg) were separated on 10% to 15% SDS-polyacrylamide gels and transferred to PVDF membranes using the wet transfer method. The blots were blocked in 5% skim milk in Tris-buffered saline/Tween-20 (TBST) and probed with primary antibodies (see the Table) followed by incubation with HRP-conjugated secondary antibodies (Cell Signaling). Finally, the proteins were quantified with ImageJ software using enhanced chemiluminescent Western blot (WB) detection reagents (EMD Millipore).

Investigative Ophthalmology & Visual Science

Real Time Quantitative PCR

Total RNA was extracted from retinas and hearts with the Trizol method (Thermo Fisher) followed by DNase treatment. RNA content was measured by Nano Drop 2000 (Thermo Fisher). The cDNA products were used as the template for quantitative PCR (qPCR), which was performed using the Quant One Step qRT-PCR Kit (SYBR Green; Takara). The specific primers were from PrimerBank, which are listed below: GAPDH (mouse) forward 5′-TGCCACTCAGAAGACTGTGG-3′ and reverse 5′-GTCCTCAGTGTAGCCCAGGA-3′; GAPDH (rat) forward 5′-AGCCAAAAGGGTCATCATCT-3′ and reverse 5′-GGGGCCATCCACAGTCTTCT-3′; CD38 (mouse) forward 5′-GAAGACTACGCCCCACTTGT-3′ and reverse 5′-ATGGGCCAGGTGTTTGGATT-3′; and CD38 (rat) forward 5′-CTGCCAGGATAACTACCGACCT-3′ and reverse 5′-CTTTCCCGACAGTGTTGCTTCT-3′. A three step reaction (95°C denature for 15 seconds, 60°C annealing for 30 seconds, and 72°C extension for 24 seconds) was carried out with the Step One Plus TM Real-time PCR System (Bio-Rad, USA). All the data were collected from the linear range of each amplification.

Statistical Analysis

All quantitative data were calculated by averaging the results of more than three samples. Microsoft Excel, Prism 6, and SPSS 17.0 statistical software were used for data processing and statistical analysis. The results are presented as the mean ± SEM. ANOVA was used to compare protein expression levels and RGC survival in multiple groups, and unpaired *t*-tests were used to compare differences in retinal thickness and EGR amplitude between two groups. $P < 0.05$ was considered statistically significant.

Results

Expression and Localization of CD38 in Retina

In 2002, Esguerra M et al. performed CD38 immunofluorescence staining of cross-sections of tiger salamander retinas and found that CD38 was predominantly present in the ganglion cell layer, the inner plexiform layer, and the inner nuclear layer of the retina. Immunolabeling of isolated retinal cells confirmed that CD38 was present only in Müller cells, and no CD38 immunoreactivity was detected in neuronal cells.[26] Müller cells are glial cells specific to the retina, accounting for more than 80% of the total retinal glial cells.[27] In this study, we further explored the expression and localization of CD38 in the retinas of rats and mice. Using the mouse heart and liver as positive controls, the WB (Figs. 1A, 1B) and qPCR (Figs. 1C, 1D) results showed that CD38 was expressed in both the rat and mouse retinas. Immunofluorescence staining revealed that CD38 was predominantly present in the ganglion cell layer, the inner plexiform layer, and the inner nuclear layer of rat and mouse retinas (Figs. 1E-1G). Furthermore, we double-stained CD38 with the Müller cell marker GS in cross-sections of mouse retinas, and the results showed that CD38 and GS could be mostly co-stained (Fig. 1H). This finding again demonstrated that CD38 is predominantly expressed in Müller cells of the retina.

CD38 Knockout Does Not Alter the Retinal Morphology or Visual Function in 8-Week-Old Mice

To explore the effect of CD38 deficiency on mouse retina, conventional CD38 KO mice were generated by crossing $CD38^{flox/flox}$ mice with EIIA-Cre mice to remove exons 2 to 3 of CD38 gene from all tissues (Fig. 2A). PCR analysis showed that CD38 gene was successfully deleted in $CD38^{-/-}$ mice (Fig. 2B). Immunofluorescence staining of CD38 in mouse retinal sections also demonstrated the success of CD38 gene KO (Fig. 2C). Rbpms immunofluorescence staining of retinal flat preparations was performed to assess the number of RGCs in wild type (WT) and $CD38^{-/-}$ mice (Fig. 2D). Quantification of the mean, central, middle, and peripheral retinal RGCs revealed no statistical differences between WT and $CD38^{-/-}$ mice (Fig. 2G). H&E staining was used to assess the retinal thickness and morphology of mice, and the results showed that there was no significant difference in the thickness and morphology of the retina between WT and $CD38^{-/-}$ mice (Fig. 2E). Image-pro Plus version 6.0 software analysis also confirmed that there was no statistically significant difference in retinal thickness between WT and $CD38^{-/-}$ mice (Fig. 2F). Furthermore, we observed that the amplitudes of dark-adapted 3.0 (Figs. 2H, 2I), dark-adapted 3.0 oscillatory potentials (Figs. 2J, 2K), and amplitude of the light-adapted 3.0 oscillatory potentials (Figs. 2L, 2M) of the electroretinograms in $CD38^{-/-}$ mice were not different from WT mice. These results indicate that CD38 deficiency did not alter the morphology and function of the retinas in mice.

CD38 Deficiency Attenuated Ischemia/Reperfusion-Induced the Glial Activation and RGCs Loss in Mouse Retinas

Studies have shown that reactive astrocytes can be strongly induced by central nervous system (CNS) injury and disease.[5] Reactive astrocytes, on the other hand, have strong neurotoxicity that ultimately induces neuronal death. Therefore, we first investigated the effect of retinal I/R injury on the induction of macroglial cells represented by astrocytes and observed the effect of CD38 loss. Immunofluorescence staining of mouse retinal sections with GFAP, a reactive macroglia marker,[28] showed that significant activation phenomena after I/R injury, such as hypertrophy of both the cell body and the macroglia projections (Fig. 3A). Activation peaked on day 3 after I/R and then gradually diminished. CD38 gene KO significantly attenuates macroglial activation caused by I/R injury. Figure 3B is a fluorescence quantification. The results showed that the relative fluorescence area of GFAP immunofluorescence staining was significantly greater in the WT + I/R day 3 group than in the WT + sham group, and significantly smaller in the KO + I/R day 3 group than in the WT + I/R day 3 group. Further quantification of retinal proteins by WB analysis showed that CD38 and GFAP protein expression increased after I/R injury and peaked on day 3 after I/R (Figs. 3C, 3D). CD38 gene KO significantly suppressed GFAP protein expression in response to I/R injury (Fig. 3E). Furthermore, the results of Rbpms fluorescence staining showed that RGCs counts at the edge, middle, and center of the retina were significantly attenuated at the peak of macroglial activation at the third day after I/R, whereas CD38 KO increased the expression to some extent (Fig. 4A). Figure 4B shows the site of

Investigative Ophthalmology & Visual Science

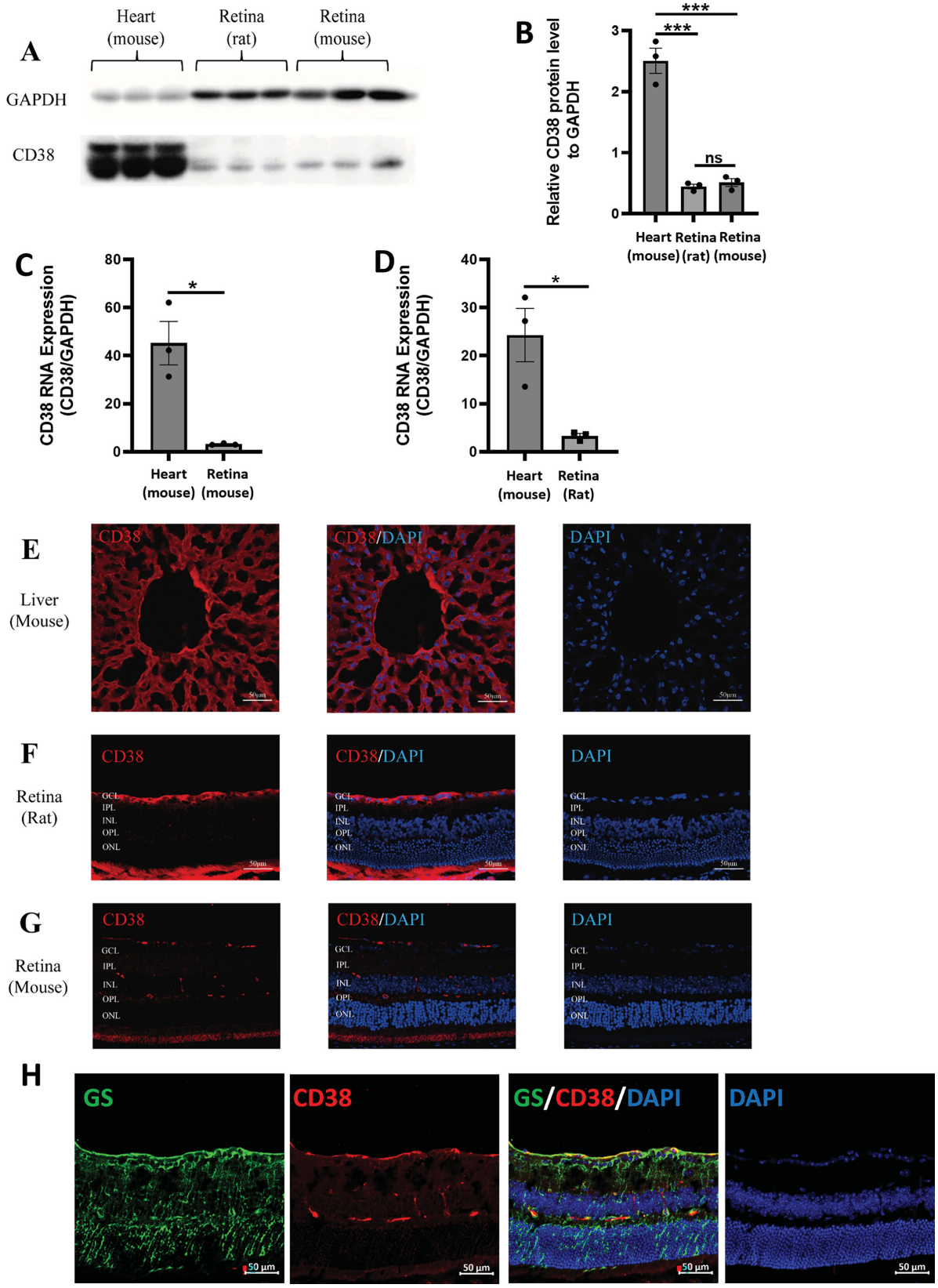

Figure 1. Expression and localization of CD38 in WT rat and mouse retinal tissues. (**A**) Detection of CD38 protein expression in mouse heart, rat retina, and mouse retina by WB. (**B**) Quantitative analysis of CD38 protein expression. (**C**) Quantitative analysis of CD38 mRNA expression in mouse retina. (**D**) Quantification of CD38 mRNA expression in rat retina. (**E**) Localization of CD38 in mouse liver by immunofluorescence. (**F**) Localization of CD38 in rat retina by immunofluorescence. (**G**) Localization of CD38 in mouse retina detected by immunofluorescence. (**H**) Cellular localization of CD38 in the mouse retina determined by GS and CD38 immunofluorescence double staining. GCL, ganglion cell layer; IPL, inner plexiform layer; INL, inner nuclear layer; OPL, outer plexiform layer; ONL, outer nuclear layer; WT, wild type; GS, marker for Müller cells; data presented as: mean ± SEM; ns, not significant; $^{*}P < 0.05$; $^{***}P < 0.001$.

Investigative Ophthalmology & Visual Science

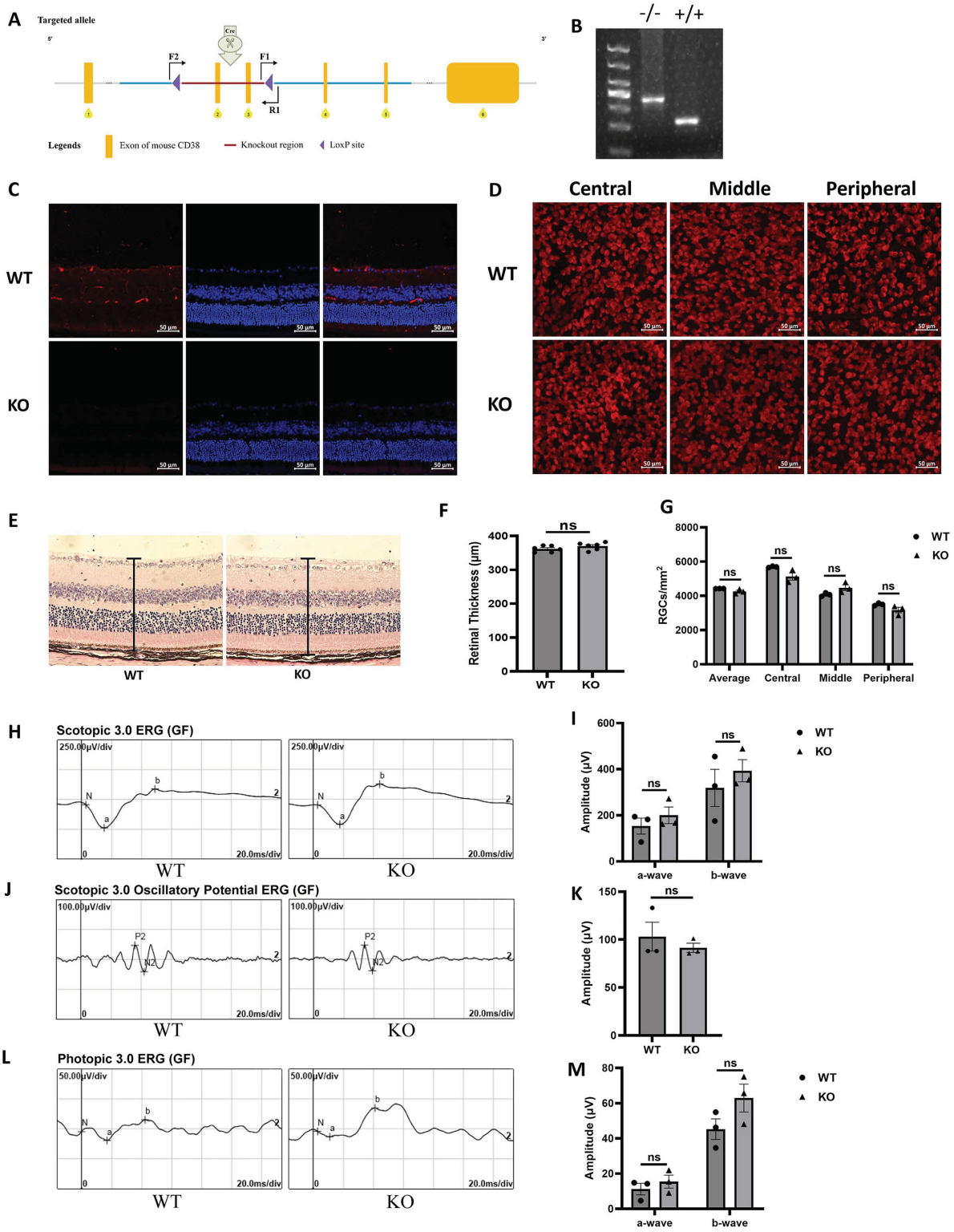

Figure 2. Identification of CD38 KO mice and assessment of retinal morphology and visual function. (**A**) CD38 gene knockout schematic. (**B**) PCR identification of CD38 KO mice. (**C**) CD38 immunofluorescence staining of retinal paraffin sections identified successful CD38 knockdown. (**D**) Immunofluorescent staining of Rbpms in retinal flat preparations for assessing the number of RGCs in WT and CD38$^{-/-}$ mice. (**E**) H&E staining of paraffin sections of retinas from WT and CD38 KO mice was observed using an inverted fluorescence microscope at a magnification of × 20. (**F**) Quantitative analysis of retinal thickness in WT and CD38 KO mice. (**G**) Quantitative statistical analysis of the average, central, middle, and peripheral RGCs in the retina of WT and CD38$^{-/-}$ mice. (**H, I**) Dark-adapted 3.0 ERG assays in WT and CD38 KO mice. (**J, K**) Dark-adapted 3.0 oscillatory potential ERG analysis in WT and CD38 KO mice. (**L, M**) Bright adapted 3.0 ERG analysis in WT and CD38 KO Mice. Peripheral, about 150 to 200 μm from the retinal margin; middle, about 700 to 800 μm from the margin; and central, about 1500 to 1600 μm from the margin; WT, wild type; KO, knockout; Rbpms, markers for RGCs; data presented as: mean ± SEM, ns, not significant.

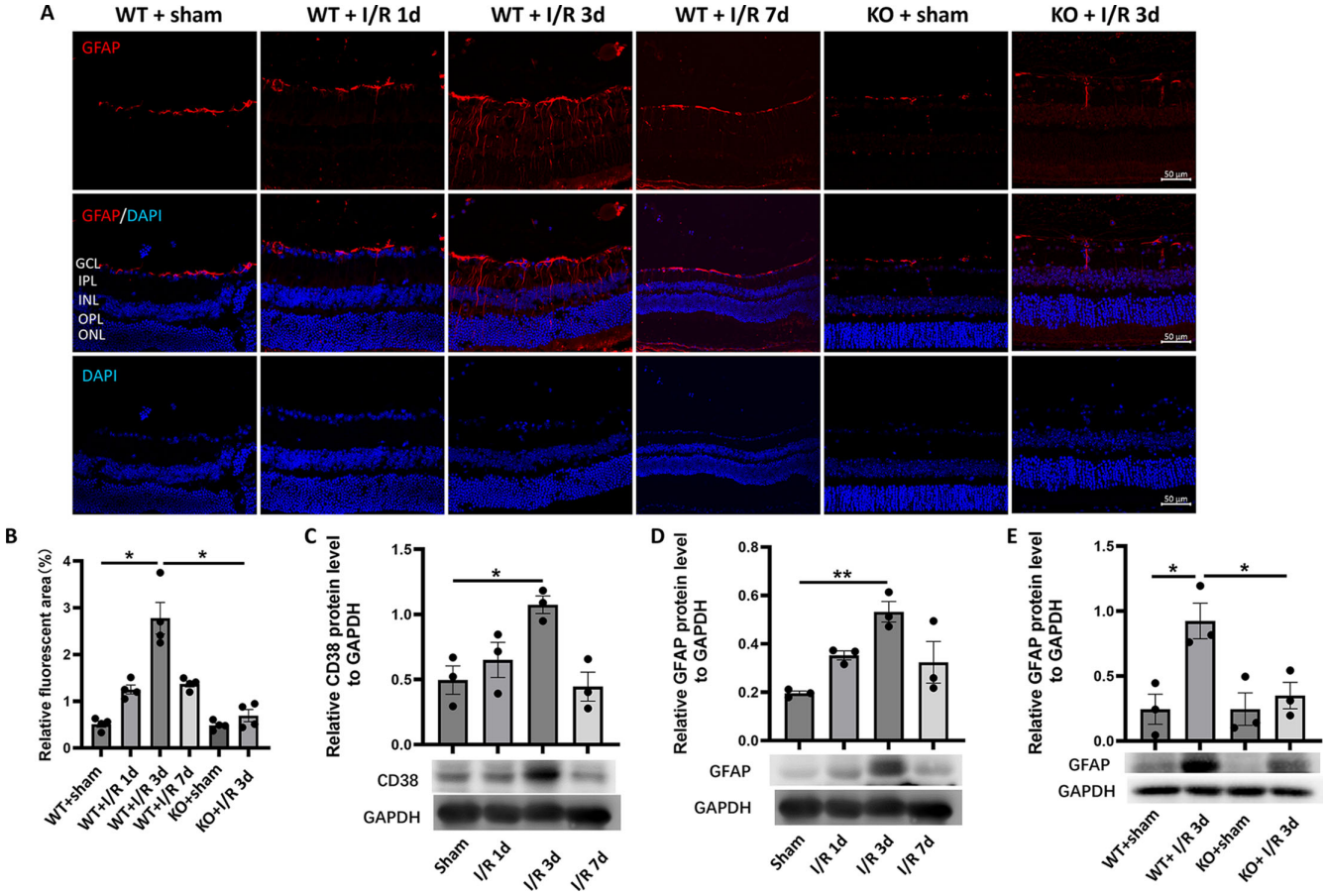

Figure 3. Effect of CD38 KO on retinal glial activation in mice in the I/R model. (**A**) GFAP immunofluorescence staining of paraffin sections of mouse retinas. (**B**) Quantitative statistics of GFAP immunofluorescence staining of paraffin sections of mouse retina. (**C**) The expression of CD38 protein in retina was detected by WB in sham operation group and I/R on day 1, day 3, and day 7. (**D**) The expression of GFAP proteins in retina was detected by WB in the sham operation group and I/R on day 1, day 3, and day 7. (**E**) WB was used to detect changes in CD38 protein expression in retinas at 3 days of I/R in WT and KO mice. GCL, ganglion cell layer; IPL, inner plexiform layer; INL, inner nuclear layer; OPL, outer plexiform layer; ONL, outer nuclear layer. Scale bars = 50 μm; WT, wild type; KO, knockout; data presented as mean ± SEM. $^{*}P < 0.05$, $^{**}P < 0.01$.

retinal image acquisition for each quadrant. Figure 4C shows a quantitative analysis of Rbpms staining in retinal preparations that showed an average decrease in of approximately 40% in RGC counts after 3 days of I/R injury, whereas CD38 KO reduced this loss to 10%. This trend was also observed at the periphery, middle, and center of the retina.

CD38 Deficiency Alleviated the Optic Nerve Crush Injury-Induced Glial Activation, Loss of RGCs and Impaired Retinal Function in Mice

We also explored macroglial activation in the ONC model and observed the effect of CD38 depletion on activation. We performed immunofluorescence staining of mouse retinal preparations using the reactive macroglia marker GFAP, and the results showed the hypertrophy of both the cell body and the macroglia projections after ONC injury. Activation peaked on day 7 after ONC injury and then gradually diminished (Fig. 5A). CD38 gene KO significantly attenuated macroglial activation caused by crush injury in the optic nerve. We also quantitatively assessed GFAP immunofluorescence staining. The statistical plot of the quantification showed that the cytosolic area of the macroglia in the WT + crush 7d group was significantly larger than that in the WT + sham group, whereas the cytosolic area in the KO + crush day 7 group was significantly smaller than that in the WT + crush day 7 group (Fig. 5B). Further quantification of retinal protein by WB showed that GFAP protein expression increased after crush injury and peaked on day 7 after injury in the optic nerve (Fig. 5C). CD38 gene KO significantly suppressed GFAP protein expression in response to ONC (Fig. 5D). Next, we observed the loss of RGCs in the ONC model. The results of Rbpms staining of flat retinal preparations showed that the fluorescence intensity of RGCs at the retinal peripheral, middle, and center was significantly attenuated at the peak of macroglia activation, that is, on day 7 after ONC injury, whereas CD38 deficiency reversed this alternation to some extent (Fig. 6A). Figure 6B shows a quantitative result of RGC counts over a time gradient following ONC injury. The results showed that the mean RGC count on the third day after ONC did not change significantly, but decreased greatly on the seventh day after crush, with a loss of approximately 60%, and further decreased by 80% by the 14th day after crush. Figure 6C shows the effect of CD38 gene knockout on RGC counts. CD38 KO reduced RGC loss to 40% on day 7 of ONC injury. This trend was observed in the periphery, middle, and center

Investigative Ophthalmology & Visual Science

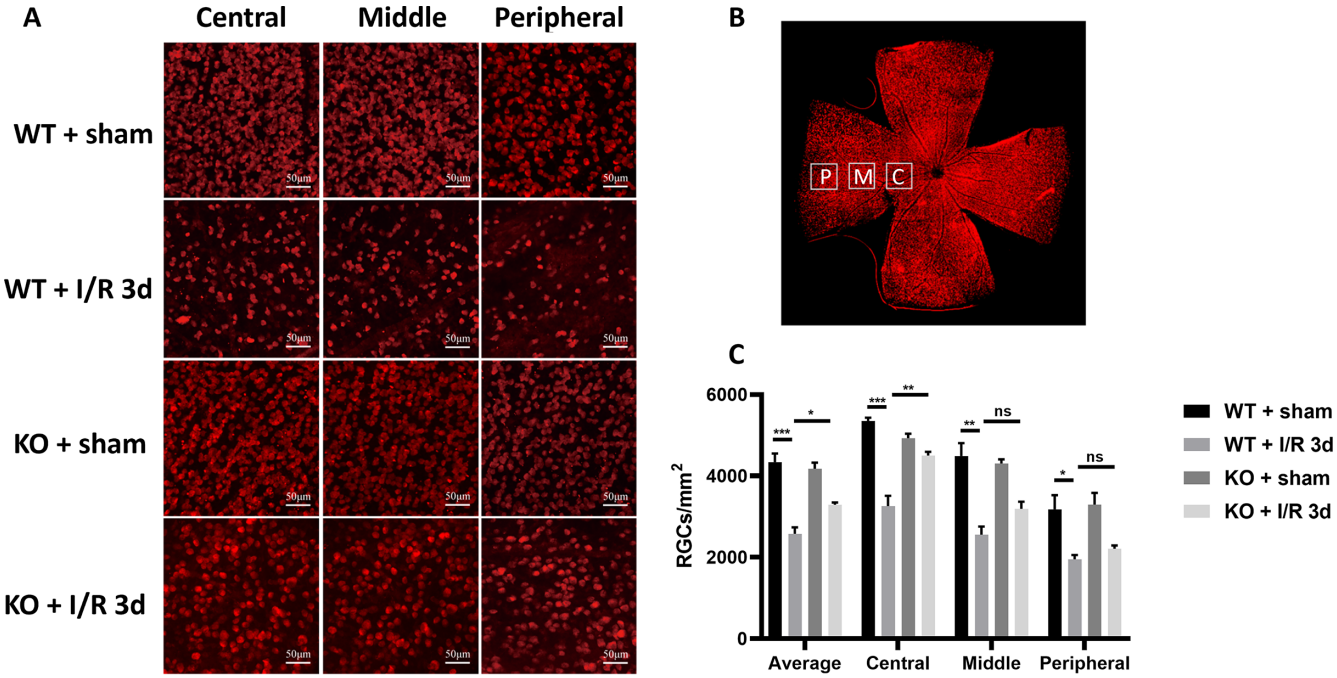

Figure 4. Effect of CD38 KO on the number of RGCs in mice in the I/R model. (**A**) Immunofluorescence staining of Rbpms in retinal flat preparations from sham WT and KO mice and I/R 3d WT and KO mice (representative images showing the central, middle, and peripheral ganglion cells in the retina). (**B**) Schematic drawing of retinal flat and counting. (**C**) Quantitative analysis of mean RGCs in the central, middle, peripheral, and whole retina. P = the peripheral, about 150 to 200 μm from the retinal margin. M = the middle, about 700 to 800 μm from the margin. C = the central, about 1500 to 1600 μm from the margin. Scale bars = 50 μm; WT, wild type; KO, knockout; data presented as: mean ± SEM; $^{*}P < 0.05$, $^{**}P < 0.01$, $^{***}P < 0.001$, $n = 4$.

of the retina. We further evaluated the effect of CD38 deficiency on retinal function. The scotopic 3.0 ERG showed that both the a-wave and b-wave amplitudes decreased after ONC injury, and CD38 knockdown could significantly alleviate the decrease in both a-wave and b-wave amplitudes induced by ONC injury (Fig. 6D). Photopic 10.0 ERG showed that both a-wave and b-wave amplitudes decreased after ONC injury, and CD38 knockdown alleviated the a-wave and b-wave amplitude decreases caused by ONC injury to some extent (Fig. 6E). This finding suggested that CD38 deletion also has a protective effect on the function of retinal optic cone optic rod cells and bipolar cells.

CD38/Sirt1 Signaling-Mediated Deacetylations of the Downstream Molecules Were Responsible for ONC Injury-Induced Inflammation and Apoptosis in Retinas of Mice

To further investigate the mechanism of the protective effect of CD38 deficiency on the retina, we assessed the expression of CD38 and the CD38-related proteins in ONC model. As shown in Figures 7A and 7B, the expression of Sirt1 protein was gradually decreased, whereas the expression of CD38 protein was gradually increased with a peak on the seventh day after crush injury in the optic nerve. In addition, we examined the expressions of the acetylated NF-κB p65 and p53 in this setting and our results showed that Ac-p65 and Ac-p53 expressions were gradually increased with a peak at day 7 after optic nerve crush injury, which was highly consistent with CD38 expression (Figs. 7C, 7D). Furthermore, our results showed that the inflammatory factor IL-1β was increased gradually increased after optic nerve crush injury with a peak on the seventh day after optic nerve crush injury (Fig. 7E), whereas the apoptotic protein Caspase3 was significantly increased after optic nerve crush injury (Fig. 7F).

CD38 Deficiency Increased the Retinal NAD+ Content and p65, p53 Deacetylation in the ONC Model

Previous results showed major changes in retinal CD38 protein expression following ONC injury, and showed high concordance with changes in Ac-p65 and Ac-p53. It is necessary to verify whether these phenomena arise due to coincidence or whether there are causative relationships. Therefore, we further explored CD38$^{-/-}$ mouse retinas. First, we examined the NAD + content in retinas from WT and CD38$^{-/-}$ mice using an NAD+ kit. The results showed that the amount of NAD+ in the retina of CD38$^{-/-}$ mice was significantly higher than that in WT mice, and the amount of NAD+ in the retina of WT mice was dramatically reduced on the seventh day of ONC injury, whereas the level of NAD+ in the retinas of CD38$^{-/-}$ mice was still maintained at a higher level (Fig. 8A). Next, we examined changes in the expression of related proteins. The results showed that the amount of Sirt1 protein in the retinas of CD38$^{-/-}$ mice was significantly greater than that of WT mice, suggesting that CD38 deficiency upregulates Sirt1 expression (Fig. 8B). The expression of Ac-p65 and Ac-p53 in the retinas of CD38$^{-/-}$ mice was significantly lower than that in WT mice on the seventh day after optic nerve crush injury (Figs. 8C, 8D), and the

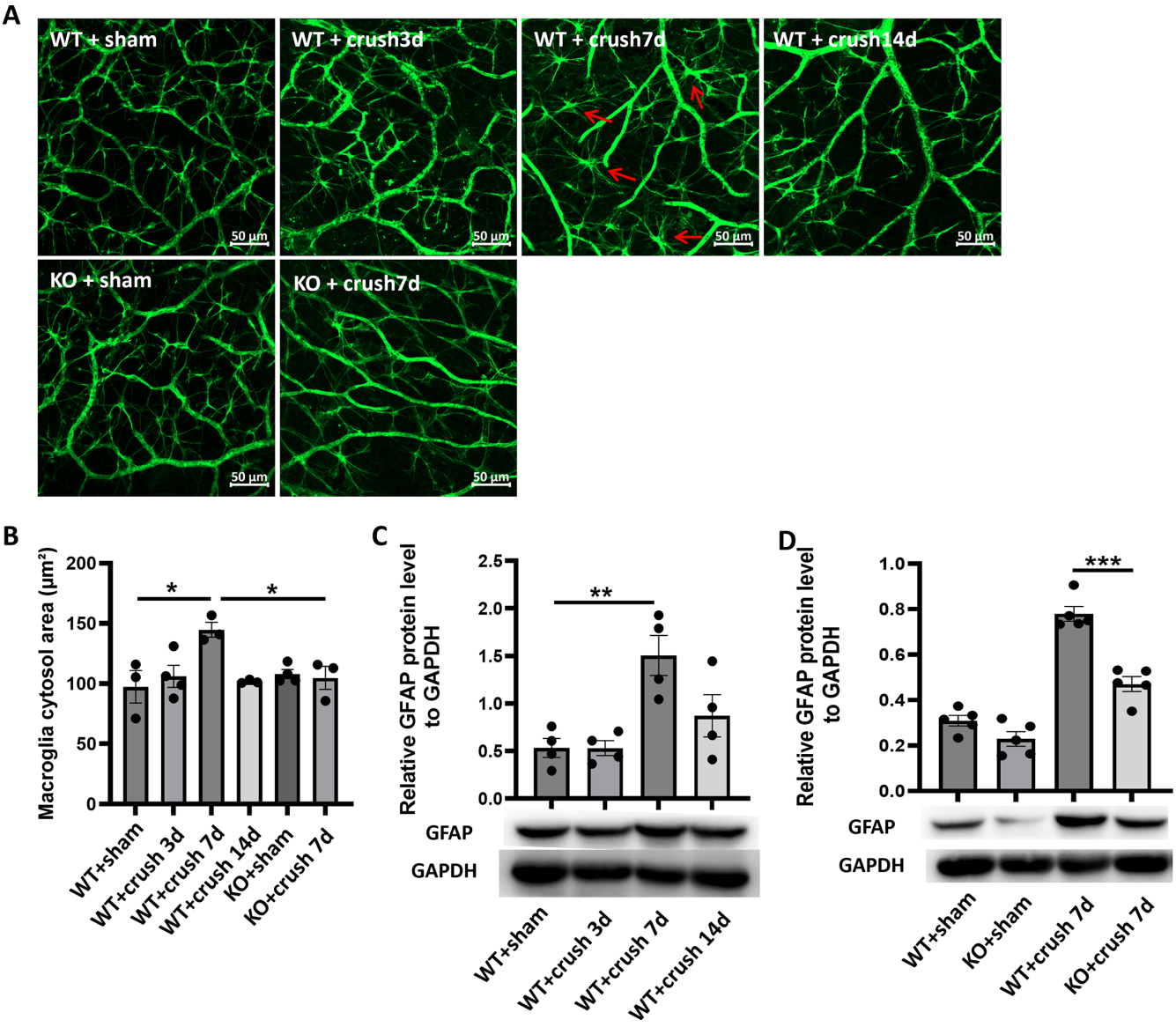

Figure 5. Effect of CD38 KO on retinal glial cell activation in mice in the ONC model. (**A**) GFAP immunofluorescence staining of mouse retinal flat preparations. (**B**) Quantitative statistics of mouse retinal flat preparations GFAP immunofluorescence staining. (**C**) The expression of GFAP protein in retina was detected by WB in sham operation group and crush on day 3, day 7, and day 14. (D) WB was used to detect changes in CD38 protein expression in the retina of sham and crush 7 day groups in WT and KO mice. The *red arrow* = activation of the macroglia, Scale bars = 50 μm; WT, wild type; KO, knockout; data presented as mean ± SEM. $^{**}P < 0.01$, $^{***}P < 0.001$.

expression of the inflammatory cytokines TNF-α and IL-1β (Figs. 8E, 8F), which are closely related to the inflammatory response, also showed a similar trend. At the same time, at the peak of Caspase3 expression, on the third day after crush injury, we observed the effect of CD38 gene KO on Caspase3 expression. The results showed that the expression of Caspase3 in the retinas of CD38$^{-/-}$ mice was significantly lower than that in the retinas of KO mice (Fig. 8G).

CD38 Deficiency Protected the Retina From ONC-Induced Injury Through Activating the NAD+/Sirt1 Signaling Pathway

From previous results, we found that the NAD+ content increased and NF-κB p65 and p53 acetylation decreased in the retinas of CD38 KO mice. Thus, it is tempting to think that CD38 KO reduces NAD+ consumption, leading to Sirt1 having a more sufficient level of NAD+ coenzyme to perform the deacetylase function, thus affecting a downstream series of deacetylation reactions and controlling the development of inflammatory responses and apoptosis. To test this hypothesis, we injected CD38$^{-/-}$ mice intraperitoneally with EX527. The EX527 can highly selectively inhibit SIRT1, with IC50 values of 60 to 100 nM, and IC50 values of 19.6 μM and 48.7 μM for the SIRT2 and SIRT3 subtypes, respectively.[29] To assess the effect of EX527 on Sirt1 activity, we examined the NAD+ content in the retina of WT mice after EX527 injection. The results are shown in Figure 9A and indicate that the NAD+ content in the retina was significantly increased after EX527 injection, suggesting that EX527 indeed reduced SIRT1 activity in the retina. Next,

Investigative Ophthalmology & Visual Science

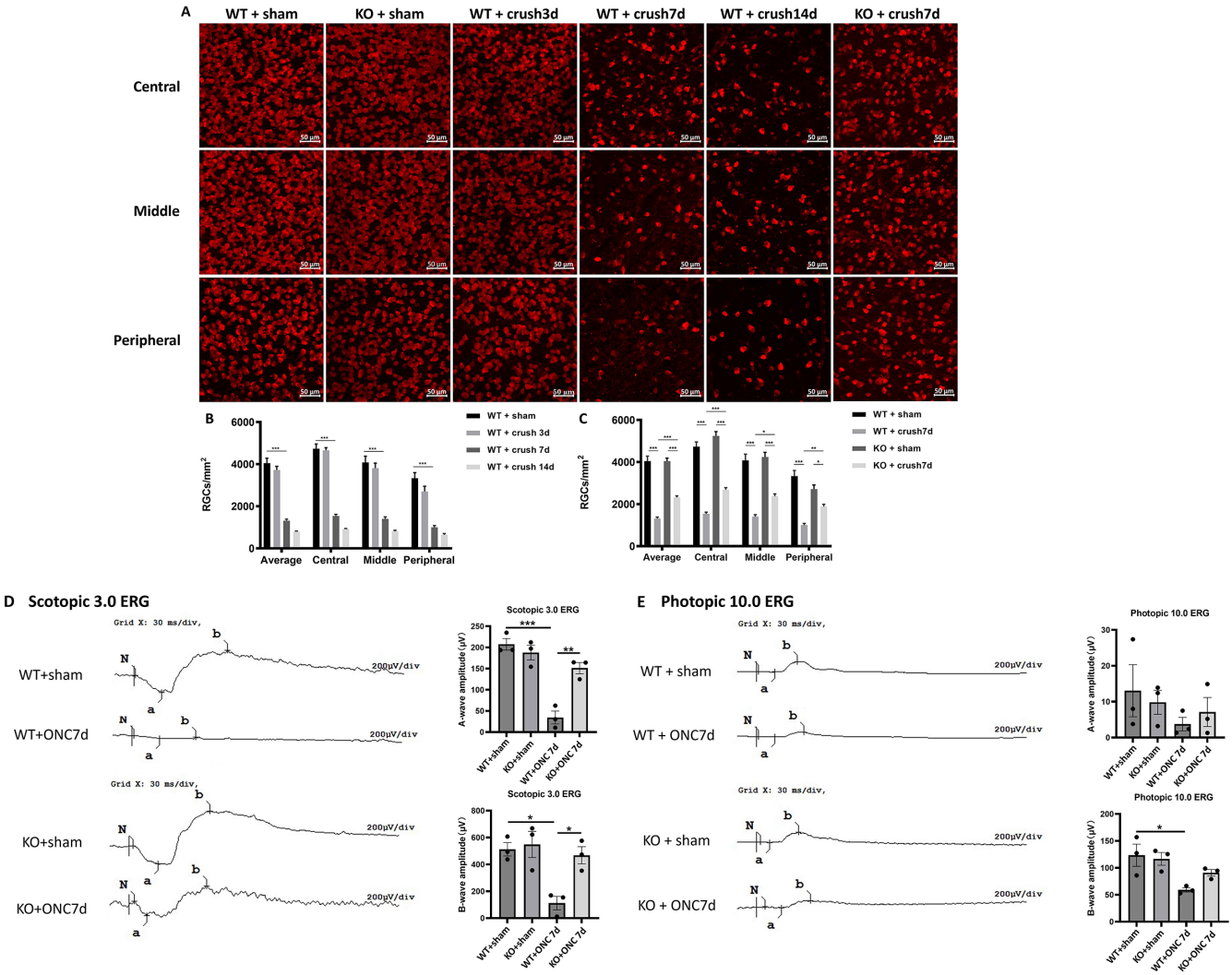

Figure 6. Effect of CD38 KO on retinal ganglion cell number and retinal function in ONC model mice. (**A**) Immunofluorescence staining of Rbpms in retinal flat preparations from WT and KO mice (representative images showing the central, middle, and peripheral ganglion cells in the retina). (**B, C**) Quantitative analysis of mean RGCs in the central, middle, peripheral, and whole retina. (**D**) Scotopic 3.0 ERG assesses retinal function in WT and CD38$^{-/-}$ mice. (**E**) Photopic 10.0 ERG assesses retinal function in WT and CD38$^{-/-}$ mice. Peripheral, about 150 to 200 μm from the retinal margin; middle, about 700 to 800 μm from the margin; central, about 1500 to 1600 μm from the margin. Scale bars = 50 μm; WT, wild type; KO, knockout; data presented as: mean ± SEM; *$P < 0.05$, **$P < 0.01$, ***$P < 0.001$.

the expression of retina-associated proteins was observed in CD38$^{-/-}$ mice with or without EX527 under the same conditions of ONC injury. The results showed that Sirt1 protein expression in the retina of crush injured mice was further reduced after EX527 administration (Fig. 9B), and, at the same time, GFAP expression of Ac-p65 and Ac-p53 protein was significantly increased (Figs. 9C-9E), and the expression of inflammatory factor TNF-α and apoptotic protein Caspase3 was also increased (Figs. 9F, 9G). Thus, we suggest that the protective effect of CD38 + KO on the mouse retina is mediated at least in part by NAD+/Sirt1.

Discussion

NAD+ is a central metabolite in maintaining a healthy nervous system, and CD38 has also aroused great concern as a major modulator of NAD+ in the brain.[30] In this study, we observed the protective effect of CD38 gene KO on RGCs in a retinal I/R model and an ONC model, and preliminarily explored the possible mechanism of this protective effect. The results showed that CD38 KO could reduce the loss of RGCs and macroglial activation in the mouse retina, and could improve the function of the retina. At the molecular level, we observed that CD38 KO reduced the acetylation of NF-κB p65 and p53 and the expression of the inflammatory cytokines IL-1β and TNFα and the apoptotic protein Caspase3 in mouse retinas and that the administration of a Sirt1 inhibitor alleviated this regulatory effect, therefore, we speculated that the protective effect of CD38 KO on RGCs may be achieved through NAD+/Sirt1.

In diseases such as glaucoma, failure to survive or RGC neurons underlies visual loss.[25] ONC is not only a useful model for traumatic optic neuropathy, but also for glaucomatous injury because it similarly induces glial activation and inflammatory factor production, and ultimately leads to RGC cell death and degeneration.[31] Similarly, retinal I/R injury is also an important pathological marker of glaucoma, central retinal arteriovenous occlusion, and other

Investigative Ophthalmology & Visual Science

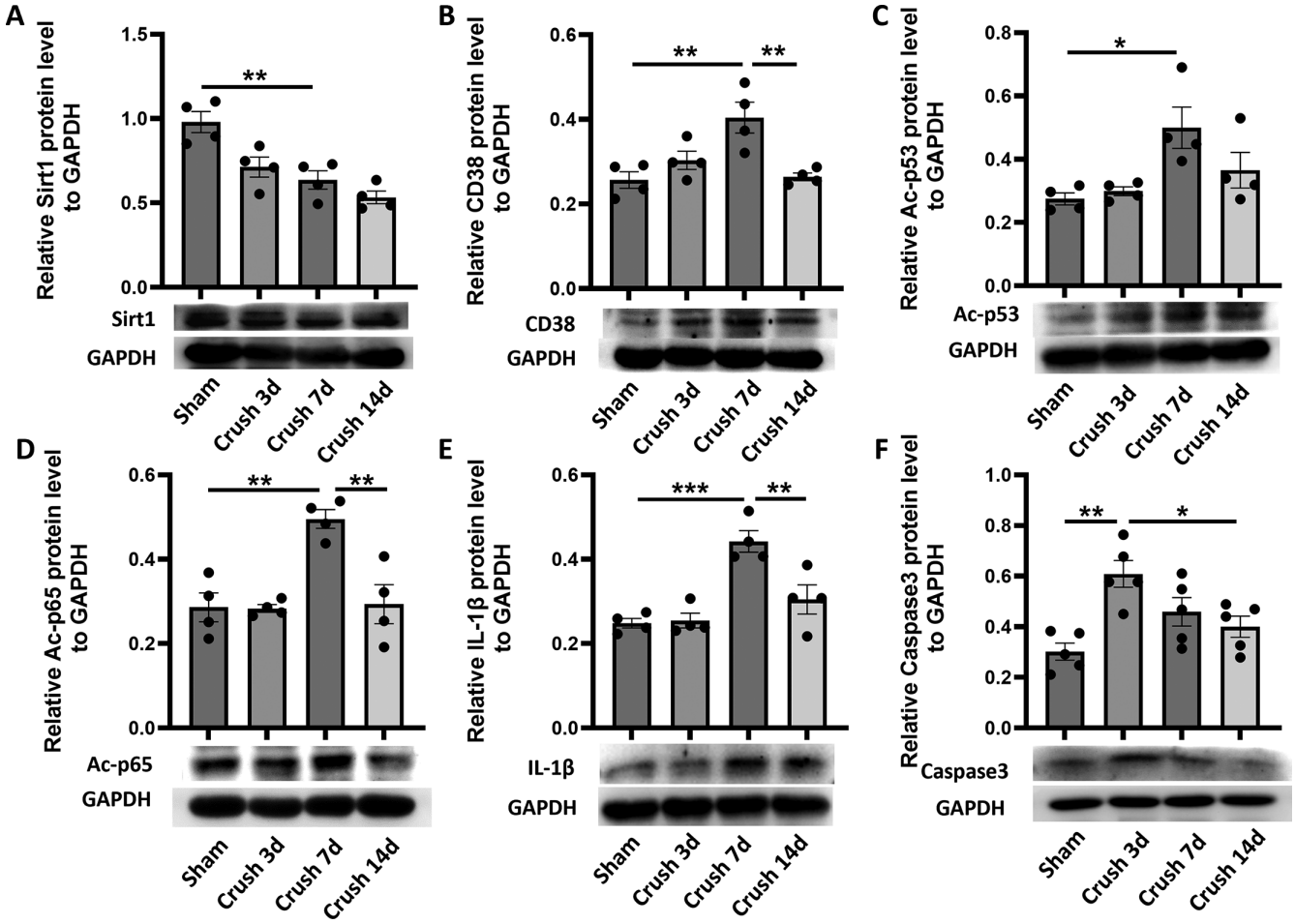

Figure 7. Changes in Sirt1 and CD38 protein expression and assessment of the degree of deacetylation of downstream molecules in the ONC model. (**A**) The expression of Sirt1 protein in retina was detected by WB in the sham operation group and crush on day 3, day 7, and day 14. (**B**) The expression of CD38 protein in retina was detected by WB in the sham operation group and crush on day 3, day 7, and day 14. (**C**) The expression of Ac-p53 protein in retina was detected by WB in the sham operation group and crush on day 3, day 7, and day 14. (**D**) The expression of Ac-p65 protein in retina was detected by WB in the sham operation group and crush on day 3, day 7, and day 14. (**E**) The expression of IL-1β protein in retina was detected by WB in the sham operation group and crush on day 3, day 7, and day 14. (**F**) The expression of Caspase3 protein in retina was detected by WB in the sham operation group and crush on day 3, day 7, and day 14. WT, wild type; KO, knockout; data presented as: mean ± SEM. *$P < 0.05$, **$P < 0.01$, ***$P < 0.001$.

related retinopathies.[32] In this study, to illustrate the problem more systematically and comprehensively and to exclude the contingency of a single model, we used both ONC and retinal I/R models. The results showed that RGCs were lost after retinal I/R and optic nerve injury. We noticed that RGC counts did not change significantly on the third day after optic nerve injury, but decreased by 60% on the seventh day, and further decreased by 80% on the 14th day compared to the sham group. This phenomenon is in good agreement with previous findings.[33] After orbital optic nerve transection in adult rats, almost all RGCs survived for 5 days, followed by sudden massive death, and the long interval between axonal injury and RGC death may be attributed to a series of molecular events, such as neurotrophic factor release triggered by axonal interruption.[34] Several recent studies have shown that some RGC types differ in their ability to survive or regenerate axons after ONC, and evaluation of some injury or regeneration susceptibility genes has revealed differences in their expression in different RGC types.[35] For example, one study reported that only approximately 20% of RGCs survived 2 weeks after ONC surgery in rats, with intrinsic photosensitive retinal ganglion cells (ipRGCs) of the M1 type accounting for 11% of all surviving cells, and that 35% to 50% of the small amount of spontaneous axonal regeneration of RGCs observed at 6 weeks postinjury was composed of ipRGCs.[36,37] On the other hand, there are several RGCs subtypes that are extremely sensitive to injury, such as ON-OFF direction-selective retinal ganglion cells (ooDSGCs) and W3-retinal ganglion cells, which are significantly less likely to survive than total RGCs after 7 days of ONC injury.[38] Moreover, there are differences in the susceptibility of different RGCs subtypes to different types of lesions.[39] This largely explains our findings that some RGCs were substantially lost after 7 days of ONC, whereas a small number of RGCs survived beyond 14 days. In addition, when we performed statistical analysis of RGC counts according to retinal peripheral, middle, and center sites separately, it was found that the degree of RGC loss at different sites was not very consistent under the same conditions. It has been shown that the loss of RGCs early in injury can be localized to specific retinal

Investigative Ophthalmology & Visual Science

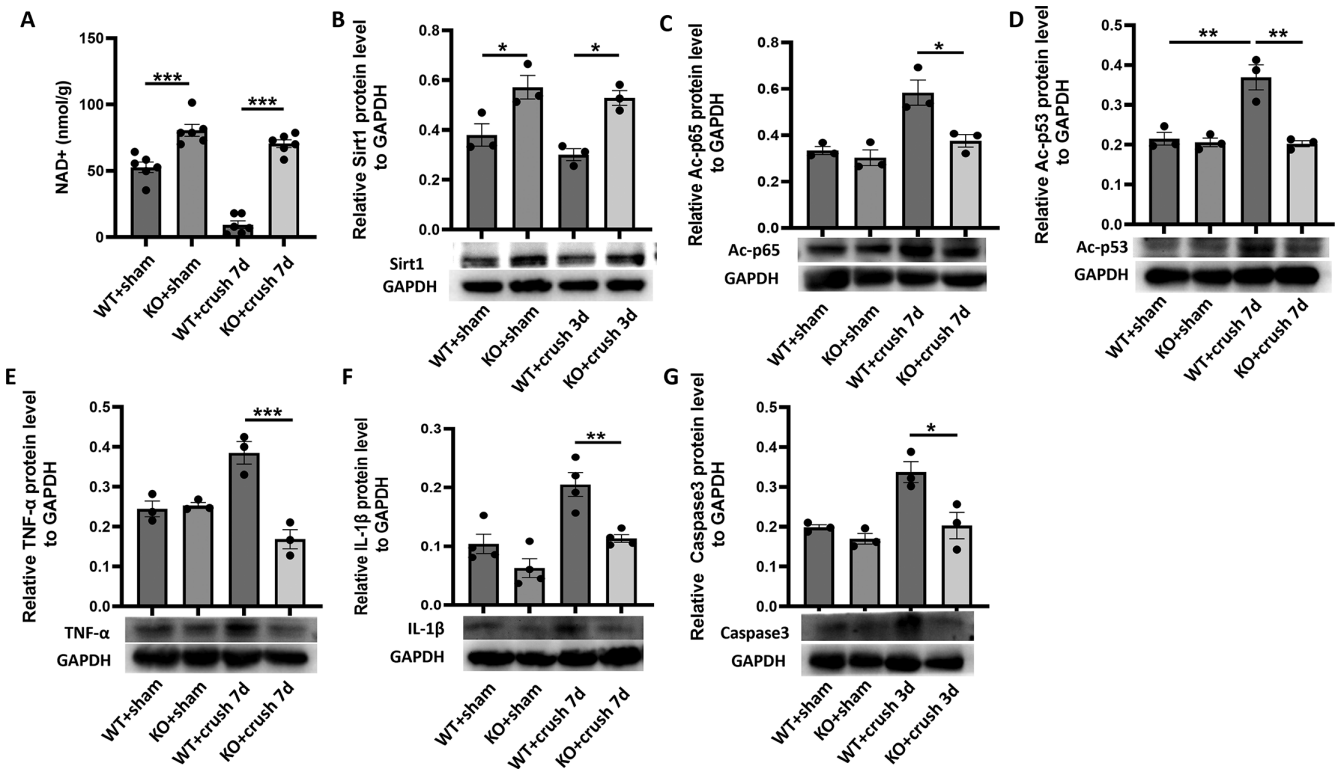

Figure 8. To evaluate the effect of CD38 deletion on NAD+ content, acetylated protein content, and inflammatory and apoptotic protein expression in the retina in the optic nerve crush model. (**A**) In the crush day 7 model, the NAD+ kit was used to detect the changes of NAD + content in the retina of WT and KO mice. (**B**) In the crush day 7 model, the expression of Sirt1 protein in the retina of WT and KO mice was detected by WB. (**C**) In the crush day 7 model, the expression of Ac-p65 protein in the retina of WT and KO mice was detected by WB. (**D**) In the crush day 7 model, the expression of Ac-p53 protein in WT and KO retinas was detected by WB. (E) In the crush day 7 model, the expression of TNF-α protein in the retina of WT and KO mice was detected by WB. (**F**) In the crush day 7 model, WB was used to detect the changes of IL-1β protein expression in the retina of WT and KO mice. (**G**) In the crush day 3 model, WB was used to detect changes in Caspase3 protein expression in the retina of WT and KO mice. WT, wild type; KO, knockout; data presented as: mean ± SEM. *$P < 0.05$, **$P < 0.01$, ***$P < 0.001$.

regions. For example, although axotomy has been reported to trigger the death of RGCs throughout the retina, the loss of RGCs was more pronounced in the central region of the retina,[40] which is very similar to our results. One possible explanation is that RGCs located in the central retina are located in the gaze region, where they experience more frequent metabolic stress due to exposure to more light, which results in them being more sensitive and not particularly resistant to subtle changes.[41,42] Whereas RGCs located in the periphery have longer axons and are likely to be surrounded by more neuroglia, they have relatively adequate structural and nutritional support, which leads to them being more stable than RGCs in the central part of the retina.[43,44] This explains the loss imbalance that occurred in that study when we artificially evaluated RGCs in the central, middle, and peripheral regions. In addition, our study assessed the activation of mouse retinal macroglia. Macroglia cells of the retina mainly include astrocytes and Müller cells, and, in glaucoma, astrocytes switch from a resting state to an activated state and act as early responders to mediate the activation of various inflammatory pathways, such as TNF-α and NF-κB.[45] In our study, retinal GFAP expression gradually increased following I/R injury and peaked on the third day after injury. The results of immunofluorescence staining of retinal sections showed that glial cells were no longer confined to the nerve fiber layer (NFL) after I/R injury, but extended into the outer plexiform layer (OPL) in a thin filamentous pattern. In the optic nerve injury model, GFAP protein expression similarly increased and peaked on day 7 postinjury. The results of GFAP staining in retinal flat preparations allowed us to observe the activation state of glial cells from another perspective different from that obtained by section staining. We observed that the cell body was significantly enlarged and the dendrites' length, number, and disorganization was increased after injury.

To elucidate the molecular mechanism of injury and to explore subsequent therapeutic strategies, we evaluated retinal protein expression after optic nerve crush injury. We found that retinal sirt1 protein expression gradually decreased with time after injury, whereas acetylated NF-κB p65 and p53 protein expression increased. Sirt1 is a member of the sirtuin family of deacetylases, which play multiple roles in apoptosis, aging, and inflammation by hydrolyzing NAD+ to reverse acetylation of lysine residues on its target protein.[46,47] Inflammatory factors produced by injury, such as iNOS, can prevent Sirt1 deacetylase activity, thereby increasing acetylation and NF-κB p65 and p53 activity in various cell types including skeletal muscle cells.[48] NF-κB is a key redox-sensitive transcription factor responsible for the transcription of proinflammatory genes.[49] It regulates the transcription of a variety of proinflammatory cytokines including tumor necrosis factor-α (TNF-α),

Investigative Ophthalmology & Visual Science

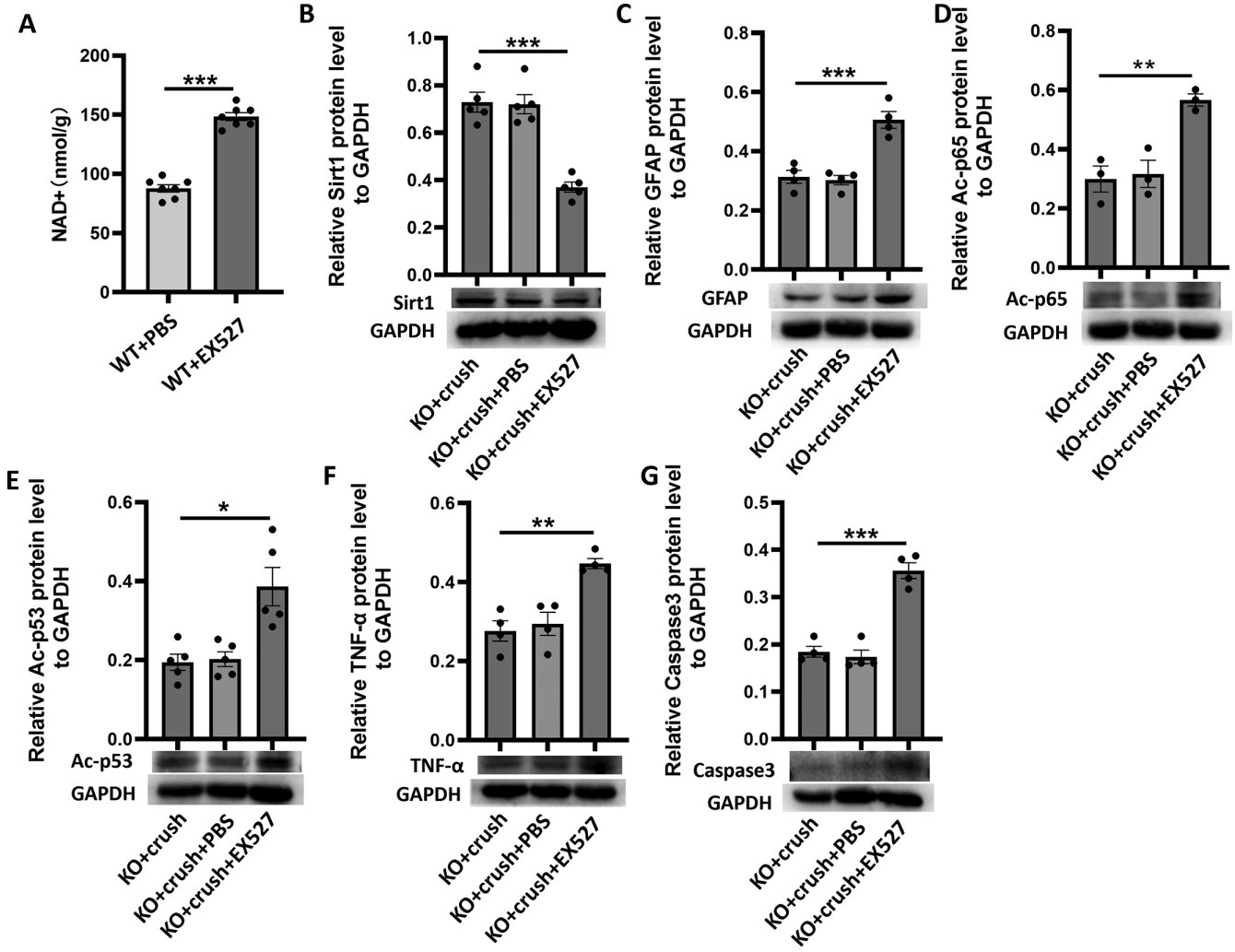

Figure 9. To assess the effect of inhibition of Sirt1 on CD38 regulation of inflammatory responses and apoptosis in the ONC model. (**A**) NAD+ kit was used to detect the changes of NAD+ content in the retina of WT mice with/without EX527. (**B**) In the crush day 7 model, WB was used to detect changes in Sirt1 protein expression in the retina of KO mice with/without EX527. (**C**) In the crush day 7 model, the changes of GFAP protein expression in the retina of KO mice were detected by WB with/without EX527. (**D**) In the crush day 7 model, the expression of Ac-p65 protein was detected by WB in the retina of KO mice in the presence/absence of EX527. (**E**) In the crush day 7 model, WB was used to detect the changes of Ac-p53 protein expression in the retina of KO mice with/without EX527. (**F**) In the crush day 7 model, WB was used to detect the changes of TNF-α protein expression in the retina of KO mice with/without EX527. (**G**) In the crush day 3 model, WB was used to detect changes in Caspase3 protein expression in the retina of KO mice in the presence/absence of EX527. EX527, Sirt1 inhibitor; PBS, EX527 vehicle; KO, knockout; data presented as: mean ± SEM. *$P < 0.05$, **$P < 0.01$, ***$P < 0.001$.

interleukin-8 (IL-8), and IL-6.[50] Sirt1 can interact with the RelA /p65 protein in NF-κB complexes, specifically deacetylating lysine 310 and enhancing the transactivation ability of NF-κB complexes.[51] It has been shown that cigarette smoke extract causes a decrease in SIRT1 levels and activity, resulting in increased acetylation and activation of RelA /p65 NF-κB, along with increased NF-κB-dependent release of proinflammatory mediators.[52] This is consistent with our study showing reduced sirt1 protein expression and increased acetylated NF-κB p65, IL-1β, and TNF-α expression following optic nerve injury. In addition, our results also showed that there was a significant increase in the expression of acetylated p53 and the apoptotic protein Caspase3 concomitant with the decrease in sirt1 following optic nerve injury. The tumor suppressor p53 has a robust apoptotic effect,[53] and it is the first identified target of SIRT1 nonhistone deacetylation.[54] Recent studies have found that SIRT1 plays an important role in neuronal survival by deacetylating p53 to inhibit apoptosis.[55]

NAD+ is involved in various cellular processes, including energy metabolism and cell signaling, and its homeostasis is determined by the balance between the activities of synthase and consumptive enzyme.[16] In addition to sirtuins, CD38 is another major NAD+ degrading enzyme in vivo. Various stimuli, such as injury- or aging-induced inflammatory factors and aging factors, upregulate CD38 in a cell-dependent manner.[56] CD38 is a 45KDa single-chain transmembrane glycoprotein localized on the cell membrane and was first observed on thymocytes and T lymphocytes.[57] However, further subsequent studies have demonstrated that CD38 is expressed almost ubiquitously. These include immune cells, which include NK cells, T cells, B cells, and monocytes. CD38 regulates cell signaling in immune cells, thereby controlling biological processes, such as cell prolif-

Investigative Ophthalmology & Visual Science

eration, differentiation, and apoptosis, and it is also involved in the entire inflammatory process, regulating migration, aggregation, adhesion, phagocytosis, antigen presentation, and antigen release.[58] In addition, CD38 is widely expressed outside the immune system, and in solid tissues, normal prostate epithelial cells, pancreatic islet cells, cardiomyocytes, and liver cells express this molecule.[59–61] CD38 expression has also been detected in many neurons, brain astrocytes, and microglia.[62] Although little is known about CD38 in the eyes, studies have reported its expression in retinal Müller cells[26] and corneas.[63] Our team's current and previous studies have found that CD38 is expressed in retinal microglia, astrocytes, and Müllerian cells.[20] In these nonimmune cells, CD38 mainly regulates calcium homeostasis through its metabolite cyclic adenosine diphosphate ribose (cADPR), which affects cellular mitochondrial function and the inflammatory response.[26,64,65] In addition, it can control the bioavailability of NAD and NAD-dependent enzyme activities by regulating the NAD pool, thus affecting a series of biological processes.[66] Upregulation of CD38 interferes with the activity of other NAD-dependent enzymes, such as sirtuins. In parallel, CD38 can inhibit sirtuins by reducing NAD levels and generating NAM, a well-characterized sirtuin inhibitor.[67] It has been shown that CD38 gene deletion or inhibition protects mice from impaired sirtuin activity, such as that resulting from a high-fat diet,[61] age-related mitochondrial dysfunction,[16] and d-galactose-induced cardiomyocyte senescence.[68] Thus, the interaction between CD38 and sirtuins is an important component of the pathophysiology of diseases associated with decreased NAD. Although this idea has been verified in various previous studies, thus far, there has been little research on the relationship among CD38, NAD+/sirt1, and their regulation of downstream molecules in the field of ophthalmic neuroprotection; thus, this is the original objective of our study design. In our study, both retinal I/R injury and optic nerve crush injury led to an increase in CD38 expression in the retina, and, in the ONC model, we found that concomitant with an increase in CD38, NAD+ content in the retina was extremely decreased, whereas Sirt1 expression was also inhibited. Double hits resulted in greatly impaired sirt1 deacetylation, as evidenced by a significant decrease in Ac-p65 and Ac-p53 and a substantial increase in the expression of the associated inflammatory cytokines TNF-α and IL-1β, and the apoptotic protein Caspase3. CD38 KO, on the other hand, greatly alleviated NAD+ depletion and restored the deacetylation function of the sirt1 moiety, and the expression of Ac-p65, Ac-p53, inflammatory factors, and apoptotic proteins was substantially reversed. At the same time, we found that CD38 KO reduced RGC loss and macroglial activation caused by retinal I/R injury and ONC injury, which we reasonably believe is closely related to the CD38 and NAD+/Sirt1 interaction. Finally, we intraperitoneally injected a sirt1 inhibitor (EX527) into CD38 KO mice in an attempt to further confirm the relationship between CD38 and sirt1 in the retina. Our results showed that EX527 increased Ac-p65 and Ac-p53 expression and upregulated the expression of the inflammatory cytokines TNF-α and IL-1β, and the apoptotic protein Caspase3 in CD38 KO ONC model mice, indicating that the protective effect of CD38 KO on the retina is at least partially achieved by NAD+/Sirt1.

Our studies using genome-wide CD38 KO mice may have several limitations. Knockdown of CD38 detrimental to the maintenance of classical activation, chemotactic signaling recruitment, and phagocytosis of macrophages and dendritic cells, thereby increasing susceptibility to pathogens.[69] CD38 is involved in neuronal development, and its knockdown can affect the number and morphology of neurons in the mouse brain.[70] In addition, CD38 plays an important role in endocrine glands, such as pancreatic islets, and nonspecific CD38 KO leads to impaired glucose tolerance in mice, which is detrimental to the maintenance of body glucose homeostasis.[71] Overall, genome-wide CD38 knockdown adversely affects the growth, development, and homeostatic maintenance of the organism under normal physiological conditions and may interfere with the accuracy of the study results. Therefore, it is necessary for us to further perform specific knockdown of CD38 in the future. In addition to CD38, other regulators of NAD+ levels, including NMNAT, SARM1, and PARPs, have been found to be closely associated with glaucomatous and neuroprotective effects. Modulating their activity is also a worthy topic for future anti-glaucoma therapy.

Overall, for the first time, we explored the relationship between CD38 and NAD+/Sirt1 in mouse retinal I/R and ONC models and preliminarily revealed the regulatory effect of CD38 on inflammation and apoptosis in the retina, and the protective effect of CD38 on RGCs. This provides new evidence for elucidating the mechanisms of optic neuropathy, such as glaucoma, and provides new ideas for further finding targets for delay or treatment.

Acknowledgments

Supported by the National Natural Science Foundation of China (Nos. 82260203) and the Talent Cultivation Program Fund of Affiliated Eye Hospital of Nanchang University (Nos. 2022X01).

Disclosure: **Y. Pang**, None; **H. Hu**, None; **K. Xu**, None; **T. Cao**, None; **Z. Wang**, None; **J. Nie**, None; **H. Zheng**, None; **H. Luo**, None; **F. Wang**, None; **C. Xiong**, None; **K.-Y. Deng**, None; **H.-B. Xin**, None; **X. Zhang**, None

References

1. Cesareo M, Ciuffoletti E, Ricci F, et al. Visual disability and quality of life in glaucoma patients. *Prog Brain Res*. 2015;221:359–374.
2. Sun D, Moore S, Jakobs TC. Optic nerve astrocyte reactivity protects function in experimental glaucoma and other nerve injuries. *J Exp Med*. 2017;214:1411–1430.
3. Wang R, Seifert P, Jakobs TC. Astrocytes in the optic nerve head of glaucomatous mice display a characteristic reactive phenotype. *Invest Ophthalmol Vis Sci*. 2017;58:924–932.
4. Nadal-Nicolás FM, Jiménez-López M, Salinas-Navarro M, Sobrado-Calvo P, Vidal-Sanz M, Agudo-Barriuso M. Microglial dynamics after axotomy-induced retinal ganglion cell death. *J Neuroinflammation*. 2017;14:218.
5. Liddelow SA, Guttenplan KA, Clarke LE, et al. Neurotoxic reactive astrocytes are induced by activated microglia. *Nature*. 2017;541:481–487.
6. Guttenplan KA, Stafford BK, El-Danaf RN, et al. Neurotoxic reactive astrocytes drive neuronal death after retinal injury. *Cell Rep*. 2020;31:107776.
7. Wu Y, Pang Y, Wei W, et al. Resveratrol protects retinal ganglion cell axons through regulation of the SIRT1-JNK pathway. *Exp Eye Res*. 2020;200:108249.
8. Pang Y, Qin M, Hu P, et al. Resveratrol protects retinal ganglion cells against ischemia induced damage by increasing Opa1 expression. *Int J Mol Med*. 2020;46:1707–1720.
9. Xu D, Liu L, Zhao Y, et al. Melatonin protects mouse testes from palmitic acid-induced lipotoxicity by attenuat-

ing oxidative stress and DNA damage in a SIRT1-dependent manner. *J Pineal Res*. 2020;69:e12690.
10. Deng Z, Sun M, Wu J, et al. SIRT1 attenuates sepsis-induced acute kidney injury via Beclin1 deacetylation-mediated autophagy activation. *Cell Death Dis*. 2021;12:217.
11. de Gregorio E, Colell A, Morales A, Marí M. Relevance of SIRT1-NF-κB axis as therapeutic target to ameliorate inflammation in liver disease. *Int J Mol Sci*. 2020;21(11):3858.
12. Mijit M, Caracciolo V, Melillo A, Amicarelli F, Giordano A. Role of p53 in the regulation of cellular senescence. *Biomolecules*. 2020;10(3):420.
13. Lautrup S, Sinclair DA, Mattson MP, Fang EF. NAD(+) in brain aging and neurodegenerative disorders. *Cell Metab*. 2019;30:630–655.
14. Verdin E. NAD^+ in aging, metabolism, and neurodegeneration. *Science*. 2015;350:1208–1213.
15. Clement J, Wong M, Poljak A, Sachdev P, Braidy N. The plasma NAD(+) metabolome is dysregulated in "normal" aging. *Rejuvenation Res*. 2019;22:121–130.
16. Camacho-Pereira J, Tarragó MG, Chini CCS, et al. CD38 dictates age-related NAD decline and mitochondrial dysfunction through an SIRT3-dependent mechanism. *Cell Metab*. 2016;23:1127–1139.
17. Malavasi F, Deaglio S, Funaro A, et al. Evolution and function of the ADP ribosyl cyclase/CD38 gene family in physiology and pathology. *Physiol Rev*. 2008;88:841–886.
18. Aksoy P, White TA, Thompson M, Chini EN. Regulation of intracellular levels of NAD: a novel role for CD38. *Biochem Biophys Res Commun*. 2006;345:1386–1392.
19. Braidy N, Poljak A, Grant R, et al. Mapping NAD(+) metabolism in the brain of ageing Wistar rats: potential targets for influencing brain senescence. *Biogerontology*. 2014;15:177–198.
20. Chen G, Yan F, Wei W, et al. CD38 deficiency protects the retina from ischaemia/reperfusion injury partly via suppression of TLR4/MyD88/NF-κB signalling. *Exp Eye Res*. 2022;219:109058.
21. Li Y, Zhu Y, Hu F, Liu L, Shen G, Tu Q. Procyanidin B2 regulates the Sirt1/Nrf2 signaling pathway to improve random-pattern skin flap survival. *Phytother Res*. 2023;37:3913–3925.
22. Li N, Wang F, Zhang Q, et al. Rapamycin mediates mTOR signaling in reactive astrocytes and reduces retinal ganglion cell loss. *Exp Eye Res*. 2018;176:10–19.
23. Luo H, Zhou M, Ji K, et al. Expression of sirtuins in the retinal neurons of mice, rats, and humans. *Front Aging Neurosci*. 2017;9:366.
24. Puyang Z, Feng L, Chen H, Liang P, Troy JB, Liu X. Retinal ganglion cell loss is delayed following optic nerve crush in NLRP3 knockout mice. *Sci Rep*. 2016;6:20998.
25. Cameron EG, Xia X, Galvao J, Ashouri M, Kapiloff MS, Goldberg JL. Optic nerve crush in mice to study retinal ganglion cell survival and regeneration. *Bio Protoc*. 2020;10(6):e3559.
26. Esguerra M, Miller RF. CD38 expression and NAD+-induced intracellular Ca+ mobilization in isolated retinal Müller cells. *Glia*. 2002;39:314–319.
27. Bringmann A, Pannicke T, Grosche J, et al. Müller cells in the healthy and diseased retina. *Prog Retin Eye Res*. 2006;25:397–424.
28. Lukowski SW, Lo CY, Sharov AA, et al. A single-cell transcriptome atlas of the adult human retina. *Embo J*. 2019;38:e100811.
29. Giampietro R, Spinelli F, Contino M, Colabufo NA. The pivotal role of copper in neurodegeneration: a new strategy for the therapy of neurodegenerative disorders. *Mol Pharm*. 2018;15:808–820.
30. Covarrubias AJ, Perrone R, Grozio A, Verdin E. NAD(+) metabolism and its roles in cellular processes during ageing. *Nat Rev Mol Cell Biol*. 2021;22:119–141.
31. Au NPB, Ma CHE. Neuroinflammation, microglia and implications for retinal ganglion cell survival and axon regeneration in traumatic optic neuropathy. *Front Immunol*. 2022;13:860070.
32. Jiang N, Li Z, Li Z, et al. Laquinimod exerts anti-inflammatory and antiapoptotic effects in retinal ischemia/reperfusion injury. *Int Immunopharmacol*. 2020;88:106989.
33. Oku H, Morishita S, Horie T, et al. P7C3 suppresses neuroinflammation and protects retinal ganglion cells of rats from optic nerve crush. *Invest Ophthalmol Vis Sci*. 2017;58:4877–4888.
34. Berkelaar M, Clarke DB, Wang YC, Bray GM, Aguayo AJ. Axotomy results in delayed death and apoptosis of retinal ganglion cells in adult rats. *J Neurosci*. 1994;14:4368–4374.
35. Tran NM, Shekhar K, Whitney IE, et al. Single-cell profiles of retinal ganglion cells differing in resilience to injury reveal neuroprotective genes. *Neuron*. 2019;104:1039–1055.e1012.
36. Bray ER, Yungher BJ, Levay K, et al. Thrombospondin-1 mediates axon regeneration in retinal ganglion cells. *Neuron*. 2019;103:642–657.e647.
37. Robinson GA, Madison RD. Axotomized mouse retinal ganglion cells containing melanopsin show enhanced survival, but not enhanced axon regrowth into a peripheral nerve graft. *Vision Res*. 2004;44:2667–2674.
38. Yang SG, Li CP, Peng XQ, Teng ZQ, Liu CM, Zhou FQ. Strategies to promote long-distance optic nerve regeneration. *Front Cell Neurosci*. 2020;14:119.
39. Gao J, Griner EM, Liu M, Moy J, Provencio I, Liu X. Differential effects of experimental glaucoma on intrinsically photosensitive retinal ganglion cells in mice. *J Comp Neurol*. 2022;530:1494–1506.
40. Boia R, Ruzafa N, Aires ID, et al. Neuroprotective strategies for retinal ganglion cell degeneration: current status and challenges ahead. *Int J Mol Sci*. 2020;21(7):2262.
41. Osborne NN, Li GY, Ji D, Mortiboys HJ, Jackson S. Light affects mitochondria to cause apoptosis to cultured cells: possible relevance to ganglion cell death in certain optic neuropathies. *J Neurochem*. 2008;105:2013–2028.
42. Osborne NN, Núñez-Álvarez C, Del Olmo-Aguado S. The effect of visual blue light on mitochondrial function associated with retinal ganglions cells. *Exp Eye Res*. 2014;128:8–14.
43. Ramírez AI, Salazar JJ, de Hoz R, et al. Quantification of the effect of different levels of IOP in the astroglia of the rat retina ipsilateral and contralateral to experimental glaucoma. *Invest Ophthalmol Vis Sci*. 2010;51:5690–5696.
44. Gallego BI, Salazar JJ, de Hoz R, et al. IOP induces upregulation of GFAP and MHC-II and microglia reactivity in mice retina contralateral to experimental glaucoma. *J Neuroinflammation*. 2012;9:92.
45. Yang X, Zeng Q, Barış M, Tezel G. Transgenic inhibition of astroglial NF-κB restrains the neuroinflammatory and neurodegenerative outcomes of experimental mouse glaucoma. *J Neuroinflammation*. 2020;17:252.
46. Lin JY, Kuo WW, Baskaran R, et al. Swimming exercise stimulates IGF1/PI3K/Akt and AMPK/SIRT1/PGC1α survival signaling to suppress apoptosis and inflammation in aging hippocampus. *Aging (Albany NY)*. 2020;12:6852–6864.
47. Zhao Y, Liu X, Zheng Y, Liu W, Ding C. Aronia melanocarpa polysaccharide ameliorates inflammation and aging in mice by modulating the AMPK/SIRT1/NF-κB signaling pathway and gut microbiota. *Sci Rep*. 2021;11:20558.
48. Nakazawa H, Chang K, Shinozaki S, et al. iNOS as a driver of inflammation and apoptosis in mouse skeletal muscle after burn injury: possible involvement of Sirt1 S-nitrosylation-mediated acetylation of p65 NF-κB and p53. *PLoS One*. 2017;12:e0170391.

Investigative Ophthalmology & Visual Science

49. Lepetsos P, Papavassiliou KA, Papavassiliou AG. Redox and NF-κB signaling in osteoarthritis. *Free Radic Biol Med*. 2019;132:90–100.
50. Hwang JW, Yao H, Caito S, Sundar IK, Rahman I. Redox regulation of SIRT1 in inflammation and cellular senescence. *Free Radic Biol Med*. 2013;61:95–110.
51. Kong P, Yu Y, Wang L, et al. circ-Sirt1 controls NF-κB activation via sequence-specific interaction and enhancement of SIRT1 expression by binding to miR-132/212 in vascular smooth muscle cells. *Nucleic Acids Res*. 2019;47:3580–3593.
52. Yao H, Chung S, Hwang JW, et al. SIRT1 protects against emphysema via FOXO3-mediated reduction of premature senescence in mice. *J Clin Invest*. 2012;122:2032–2045.
53. Ong ALC, Ramasamy TS. Role of Sirtuin1-p53 regulatory axis in aging, cancer and cellular reprogramming. *Ageing Res Rev*. 2018;43:64–80.
54. Luo J, Nikolaev AY, Imai S, et al. Negative control of p53 by Sir2alpha promotes cell survival under stress. *Cell*. 2001;107:137–148.
55. Li M, Li SC, Dou BK, et al. Cycloastragenol upregulates SIRT1 expression, attenuates apoptosis and suppresses neuroinflammation after brain ischemia. *Acta Pharmacol Sin*. 2020;41:1025–1032.
56. Zeidler JD, Hogan KA, Agorrody G, et al. The CD38 glycohydrolase and the NAD sink: implications for pathological conditions. *Am J Physiol Cell Physiol*. 2022;322:C521–C545.
57. Bhan AK, Reinherz EL, Poppema S, McCluskey RT, Schlossman SF. Location of T cell and major histocompatibility complex antigens in the human thymus. *J Exp Med*. 1980;152:771–782.
58. Piedra-Quintero ZL, Wilson Z, Nava P, Guerau-de-Arellano M. CD38: an immunomodulatory molecule in inflammation and autoimmunity. *Front Immunol*. 2020;11:597959.
59. Kramer G, Steiner G, Födinger D, et al. High expression of a CD38-like molecule in normal prostatic epithelium and its differential loss in benign and malignant disease. *J Urol*. 1995;154:1636–1641.
60. Boslett J, Hemann C, Christofi FL, Zweier JL. Characterization of CD38 in the major cell types of the heart: endothelial cells highly express CD38 with activation by hypoxia-reoxygenation triggering NAD(P)H depletion. *Am J Physiol Cell Physiol*. 2018;314:C297–C309.
61. Xie L, Wen K, Li Q, et al. CD38 deficiency protects mice from high fat diet-induced nonalcoholic fatty liver disease through activating NAD(+)/sirtuins signaling pathways-mediated inhibition of lipid accumulation and oxidative stress in hepatocytes. *Int J Biol Sci*. 2021;17:4305–4315.
62. Guerreiro S, Privat AL, Bressac L, Toulorge D. CD38 in neurodegeneration and neuroinflammation. *Cells*. 2020;9(2):471.
63. Sizzano F, Durelli I, Lusso R, Deaglio S, Horenstein A. Identification of the ectoenzyme-receptor CD38 on human corneal epithelial cells. *21st European Immunogenetics and Histocompatibility Conference*, 2007.
64. Roboon J, Hattori T, Ishii H, et al. Inhibition of CD38 and supplementation of nicotinamide riboside ameliorate lipopolysaccharide-induced microglial and astrocytic neuroinflammation by increasing NAD(). *J Neurochem*. 2021;158:311–327.
65. Walkon LL, Strubbe-Rivera JO, Bazil JN. Calcium overload and mitochondrial metabolism. *Biomolecules*. 2022;12(12):1891.
66. Luo H, Zhuang J, Hu P, et al. Resveratrol delays retinal ganglion cell loss and attenuates gliosis-related inflammation from ischemia-reperfusion injury. *Invest Ophthalmol Vis Sci*. 2018;59:3879–3888.
67. Tarragó MG, Chini CCS, Kanamori KS, et al. A potent and specific CD38 inhibitor ameliorates age-related metabolic dysfunction by reversing tissue NAD(+) decline. *Cell Metab*. 2018;27:1081–1095.e1010.
68. Wang LF, Cao Q, Wen K, et al. CD38 deficiency alleviates D-galactose-induced myocardial cell senescence through NAD(+)/Sirt1 signaling pathway. *Front Physiol*. 2019;10:1125.
69. Glaría E, Valledor AF. Roles of CD38 in the immune response to infection. *Cells*. 2020;9(1):228.
70. Nelissen TP, Bamford RA, Tochitani S, et al. CD38 is required for dendritic organization in visual cortex and hippocampus. *Neuroscience*. 2018;372:114–125.
71. Kato I, Yamamoto Y, Fujimura M, Noguchi N, Takasawa S, Okamoto H. CD38 disruption impairs glucose-induced increases in cyclic ADP-ribose, [Ca2+]i, and insulin secretion. *J Biol Chem*. 1999;274:1869–1872.

Investigative Ophthalmology & Visual Science